Laser and Particle Beams (2007), *25*, 639–647. Printed in the USA.

DOI: 10.1017/S0263034607000766

Prospects of high energy density physics research using the CERN super proton synchrotron (SPS)

N.A. TAHIR,[1] R. SCHMIDT,[2] M. BRUGGER,[2] I.V. LOMONOSOV,[3] A. SHUTOV,[3] A.R. PIRIZ,[4] S. UDREA,[5] D.H.H. HOFFMANN,[5] AND C. DEUTSCH[6]

[1]Gesellschaft für Schwerionenforschung Darmstadt, Darmstadt, Germany
[2]CERN-AB, Geneva, Switzerland
[3]Institute for Problems of Chemical Physics, Chernogolovka, Russia
[4]E.T.S.I. Industriales, Universidad de Castilla-La Mancha, Ciudad Real, Spain
[5]Institut für Kernphysik, Technische Universität Darmstadt and Gesellschaft für Schwerionenforschung Darmstadt, Darmstadt, Germany
[6]Laboratoire de Physique des Gaz et des Plasmas, Universite Paris-Sud, Orsay, France

(RECEIVED 30 August 2007; ACCEPTED 6 October 2007)

Abstract

The Super Proton Synchrotron (SPS) will serve as an injector to the Large Hadron Collider (LHC) at CERN as well as it is used to accelerate and extract proton beams for fixed target experiments. In either case, safety of operation is a very important issue that needs to be carefully addressed. This paper presents detailed numerical simulations of the thermodynamic and hydrodynamic response of solid targets made of copper and tungsten that experience impact of a full SPS beam comprized of 288 bunches of 450 GeV/c protons. These simulations have shown that the material will be seriously damaged if such an accident happens. An interesting outcome of this work is that the SPS can be used to carry out dedicated experiments to study High Energy Density (HED) states in matter.

Keywords: CERN SPS beams; High energy density physics; Strongly coupled plasmas

1. INTRODUCTION

The study presented in this paper has been motivated by previous work on the machine protection systems for the CERN Large Hadron Collider (LHC). The LHC will allow for collisions between two 7 TeV/c opposing proton beams, each comprising at nominal intensity 2808 bunches with 1.15×10^{11} protons per bunch. The energy stored in each beam when operating at 7 TeV/c is about 360 MJ, sufficient to melt 500 kg of copper.

One of the worst case failure scenarios, an accidental release of the entire LHC beam energy into equipment, has been considered in Tahir *et al.* (2005*a*). The damage has been estimated for a solid copper target hit at normal incidence by the full LHC beam. If instantaneous energy deposition was assumed, the energy density deposited in the material would exceed the energy that is required for vaporization by several orders of magnitude. However, the beam energy is deposited over 86 μs, long enough to change the density of the target material. This density change strongly affects the energy deposition of the impacting beam. The calculations indicate that the target density around the beam axis can be reduced by more than a factor of 10 within 2.5 μs. The material in this hot inner zone is in a plasma state, with the surrounding target in a liquid state. The density is reduced by a factor of 10 after only 100 LHC bunches out of 2808 have been delivered. The protons in the following bunches will therefore penetrate into the target more deeply as they will encounter material with reduced density — the penetration depth is estimated at up to 40 m.

One important outcome of this work has been that the LHC can also be used for high energy density (HED) matter research (Tahir *et al.*, 2005*b*). HED states in matter is a very important subject with very wide applications to numerous fields in basic and applied physics, as well as it has great potential for different important industrial applications (Tahir *et al.*, 1999, 2000*a*, 2000*b*, 2001*a*, 2001*b*, 2003*a*, 2003*b*, 2005*c*, 2005*d*, 2006, 2007*a*; Piriz *et al.*, 2002, 2003*a*, 2003*b*, 2006, 2007*a*, 2007*b*; Temporal *et al.*, 2003, 2005; Lopez Cela *et al.*, 2006; Hoffmann *et al.*, 2005).

The beams for the LHC are pre-accelerated in the Super Proton Synchroton (SPS) to 450 GeV/c and transferred to LHC via two beam lines. Several SPS cycles are required to

Address correspondence and reprint requests to: N. A. Tahir, Gesellschaft für Schwerionenforschung Darmstadt, Planckstrasse 1, 64291 Darmstadt, Germany. E-mail: n.tahir@gsi.de

fill the LHC, in one cycle, a batch with up to 288 bunches can be accelerated. Such batches are extracted from the SPS by a fast kicker magnet and transferred via a 3 km long beam line to the LHC injection point. Another fast kicker magnet deflects the beam into the LHC. Although the energy stored in the batch is less than 1% of the LHC beam at 7 TeV/c, it is enough to cause considerable damage in case of failure. Protection must start during acceleration in the SPS and must be efficient at the moment of extraction from the SPS toward the LHC throughout the LHC cycle.

During high intensity extraction tests in 2004, an incident occurred that demonstrated the damage potential of the SPS beams (Goddard *et al.*, 2005). A failure in the extraction septum magnet led to the beam being deflected into a vacuum chamber of a magnet in the transfer line from SPS to CNGS/LHC that was badly damaged as a result. The beam was a 450 GeV/c full LHC injection batch of 3.4×10^{13} protons in 288 bunches extracted with the wrong trajectory. A dedicated experiment was carried out trying to damage material in a controlled way with such a beam (Kain *et al.*, 2005), to cross-check the validity of detailed energy deposition simulations, and the assumption for the damage levels. The impact of a 450 GeV/c beam extracted from the SPS on a specially designed high-Z target was simulated for a simple geometry comprising several typical materials used for LHC equipment. The beam intensities for the test were chosen to exceed the damage limits of parts of the target, between 2×10^{12} and 8×10^{12} protons. The transverse r.m.s. beam dimensions were about 1 mm. The geometry of the target was modeled and the target heating was estimated. The temperature rise was obtained from the energy deposition using the temperature dependent heat capacity for each material. The results of the controlled damage test show reasonable agreement with the simulations.

Another experiment was performed to validate the performance of collimators with carbon composite (CC) jaws for the LHC collimation system (Ass-mann, Private communication). The length of the beam pulse was 7 μs and the transverse size of the extracted beam was about 1 mm. It is interesting to note that the 2 MJ of extracted energy corresponds to the full Tevatron beam or 0.5 kg of TNT. The LHC collimator was designed to survive a direct beam impact at twice this energy. Robustness considerations included the CC jaw, metallic support parts, and the water circuit at the CC jaw. The collimator was repeatedly hit with the 2 MJ beam (10 times at highest intensity) with distances up to 5 mm from the jaw edge. The robustness of the collimator jaw was confirmed, but a careful analysis of the collimator assembly showed a slight deformation of the jaws by a fraction of mm that lead to an improvement of the supporting structure. A robustness test was repeated and no deformation was measured (Assman, private communication).

The motivation for the studies presented in this paper is threefold: What damage is expected if the full SPS beam hits heavy Z material? (2) Is tunneling of beams through target material expected with the SPS beam? (3) Is the SPS beam powerful enough to address physics of High Energy Density Matter?

To answer the above questions, we have considered cylindrical targets made of solid copper and solid tungsten, respectively, that are irradiated with a full SPS beam. The FLUKA code described in Section 3 has been used to calculate the energy deposition in the target material by the protons and the secondary particles, and this data is used as input to a two-dimensional hydrodynamic code, BIG-2 (Fortov, 1996), to study the thermodynamic and hydrodynamic response of the heated targets.

In Section 2, we describe the CERN SPS while the energy deposition code FLUKA is discussed in Section 3. The two-dimensional hydrodynamic code BIG-2 is presented in Section 4, together with the semi-empirical equation-of-state (EOS) model that has been used to treat different material phases that are generated in the target due to beam-heating. The simulation results are discussed in Section 5, and the conclusions drawn from this work are noted in Section 6.

2. SPS AT CERN

The SPS is used as a LHC injector, but also to accelerate and extract protons and ions for fixed target experiments, and for producing neutrinos (CNGS). In particular, the risks during the fast extraction of LHC and CNGS beams must be considered since any failure during this process can lead to serious equipment damage.

The SPS accelerator has 6.9 km circumference and accelerates protons from 14 GeV/c or 26 GeV/c to a momentum of up to 450 GeV/c. It is a cycling machine with cycles length of about 10 s. The transverse beam size is largest at injection and decreases with the square root of the beam energy during acceleration. For the operation as a synchrotron, the beam size at top energy is typically on the order of 1 mm.

When the SPS operates as LHC injector, up to 288 bunches are accelerated, each bunch with about 1.1×10^{11} protons. The bunch length is 0.5 ns and two neighboring bunches are separated by 25 ns so that the duration of the entire beam is about 7 μs. The normalized emittance is 3.75×10^{-6}m. Assuming a beta function of 100 m, the beam size is 0.88 mm. When the SPS was used as proton-antiproton collider, the luminosity was maximized by minimizing the beta function to 0.5 m. Assuming this value, the beam size would be about 0.06 mm.

3. ENERGY DEPOSITION COMPUTER CODE FLUKA

High-energy protons impinging on the studied material samples produce particle cascades, depositing their energy in matter that leads to an increase in temperature. The required energy deposited by the 450 GeV/c SPS beam as a function of material and geometry, has been calculated using the FLUKA code (Fasso *et al.*, 2003, 2005). This is

a fully integrated particle physics and multi-purpose Monte Carlo simulation package, capable of simulating all components of the particle cascades in matter up to TeV energies. FLUKA has many applications in high energy experimental physics and engineering, shielding, detector and telescope design, cosmic ray studies, dosimetry, medical physics and radio-biology, as well as allows to simulate the interaction of beams with matter over a very wide energy range. The most relevant energy range for these applications being: (1) Hadron and ion beams from as low as a few MeV/u up to 10000 TeV/u. (2) Neutrons down to thermal energies. (3) Electromagnetic radiation from 1 keV up to 10000 TeV. (4) Muons up to 10000 TeV.

Neutron transport and interactions below 20 MeV are treated using a coupled 72 neutron group—22 gamma group library. Above 20 MeV for neutrons, and at all energies for the other particles, the time evolution of nuclear interactions in the models embedded in FLUKA is organized according to the following scheme: (1) Glauber-Gribov cascade (not present below a few GeVs); (2) Generalized IntraNuclear cascade (GINC, not present below 50 MeV); (3) Preequilibrium emission; (4) Evaporation/Fission/Fragmentation; (5) Gamma deexcitation.

Individual hadron-nucleon interactions, which are relevant as soon as the threshold for explicit GINC is passed, are described according to: (1) Elastic and charge exchange scattering according to phase-shift analyses (up to few GeVs) and to eikonal models at higher energies; (2) Particle production according to resonance production and decay up to a few GeVs, and according to a quark-string model (dual parton model) DPM at higher energies.

More details about the applied models and their performances, as well as a vast amount of benchmarking can be found in Fasso *et al.* (1993) and Ferrari & Sala, (1996). It is to be noted that the models used in FLUKA, also include nuclear size correction to the stopping power at very high energies.

For the purpose of the study presented in this paper, the geometry for the FLUKA calculation was a simple cylinder of solid copper and tungsten, respectively, having a radius of 5 cm, and a length of 2 m. The FLUKA simulations were made assuming solid densities and the energy deposition was obtained using realistic two-dimensional SPS beam distributions, namely, a Gaussian beam with different beam sizes (horizontal and vertical sigma was the same) values of a 0.088 mm, 0.28 mm, and 0.88 mm, respectively. The 450 GeV/c beam was incident perpendicular to the front face of the cylinder and the distribution of local energy deposition was calculated for a cylindrical symmetric three-dimensional mesh (bin size radial: 0.1 mm, longitudinal: 10 mm). The results are presented below.

Figure 1a shows specific energy deposited in copper by one bunch (1.1×10^{11} protons) along the target length at $r = 0.0$, whereas Fig. 1b shows the same variable, but in radial direction at length, $L = 10$ cm (point of maximum deposition). It is seen that a maximum specific energy of about 140 J/g is deposited in solid copper by one bunch of the SPS beam.

Figures 2a and 2b show the same variables as Figures 1a and 1b, respectively, but for a tungsten target. It is seen that in this case, a maximum energy of about 400 J/g is deposited in the target.

4. TWO-DIMENSIONAL HYDRODYNAMIC COMPUTER CODE BIG-2 AND SEMI-EMPIRICAL EOS MODEL

The computer code BIG-2 (Fortov *et al.*, 1996) is based on a Godunov type scheme that has a second order accuracy in space for solving the hydrodynamic equations. It uses a rectangular mesh with moving grids and can handle complicated beam-target configurations. It includes full particle tracking treatment for energy loss of heavy ions in matter. Moreover, the code has an option to read the energy loss data for the protons and the cascade particles as provided by the FLUKA code. Thermal conduction is also included and different phases of matter encountered as a result of

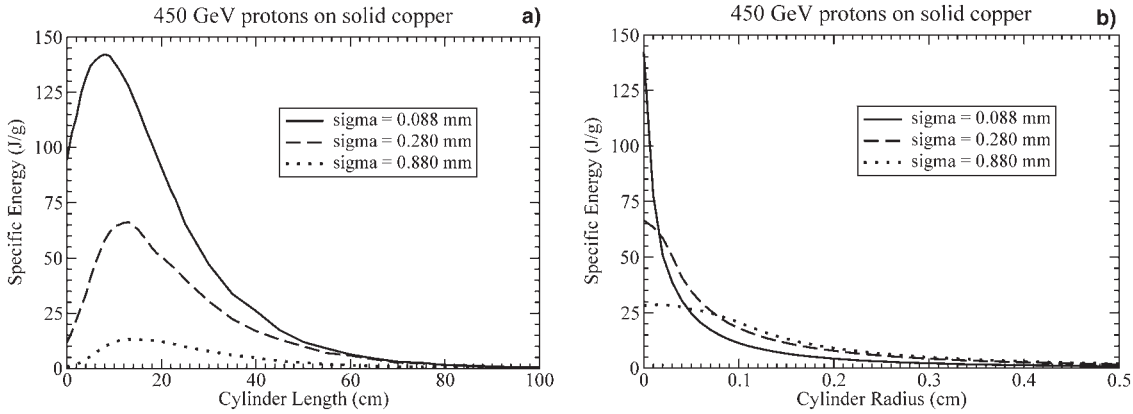

Fig. 1. Cylindrical copper target, length = 2 m, radius = 5 cm, FLUKA simulations, specific energy deposited by a single proton bunch using three different values of beam focal spot, (**a**) along longitudinal direction at r = 0.0 and (**b**) along radial direction at L = 10 cm.

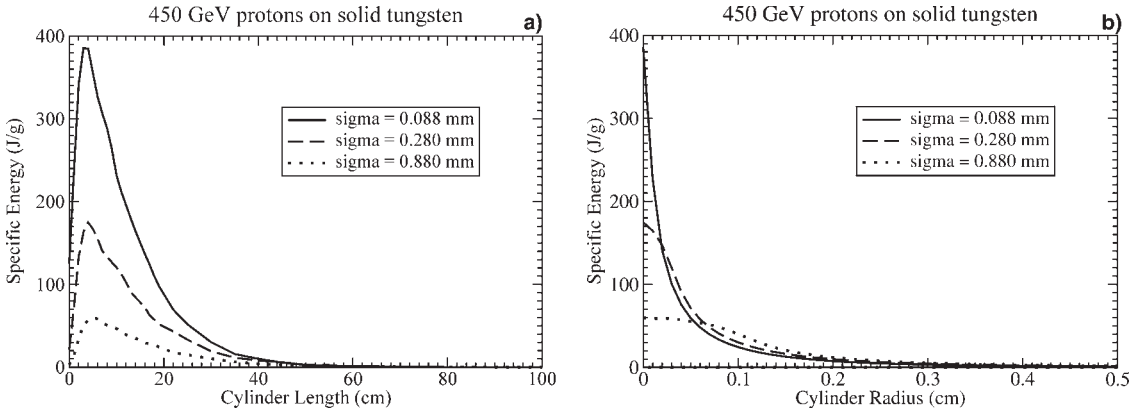

Fig. 2. Cylindrical tungsten target, length = 2 m, radius = 5 cm, FLUKA simulations, specific energy deposited by a single proton bunch using three different values of beam focal spot, (**a**) along longitudinal direction at r = 0.0 and (**b**) along radial direction at L = 10 cm.

target heating are treated using a sophisticated semi-empirical EOS model described below.

4.1. Semi-empirical EOS model

We used in numerical modeling, the wide-range multi-phase EOS for copper and tungsten. It is based on the semi-empirical model (Lomonosov, 2007), which represents further development of the model and the approach proposed in Bushman *et al.* (1993). This EOS fully assigns the free energy thermodynamic potential for metals over the entire phase diagram region of practical interest. It accounts for solid, liquid, plasma states, as well as two-phase regions of melting and evaporation. The free energy potential in the EOS model is given by the sum of the elastic contribution at $T = 0$ K and the thermal contribution by atoms and electrons. These analytic formulae represent correct theoretical results obtained for solid, liquid, or plasma domains. For example, the elastic contribution is fitted to Thomas-Fermi theory at extreme pressures, as well as to tabular value of the cohesion energy, the thermal contribution of atoms uses Debay theory for solids, anharmonicty and melting effects, and results of Monte Carlo and molecular dynamics modeling for liquid state, the thermal contribution of electrons provides for exact description of degenerated electron gas, as well as effects of first and second ionizations and many others, see Lomonosov (2007) for details. Some at the coefficients in EOS, included in the analytical expressions, are characteristic constants for each metal (atomic weight and charge, density at normal conditions, and other), and are found from tabular data, while the rest serve as fitting parameters, and their values are found from the optimum description for the available experimental, and theoretical data, and providing for correct asymptotes to calculations on the base of Debay-Hukkel and Thomas-Fermi theories.

It should be emphasized that, even though the number of coefficients in the EOS model (Lomonosov, 2007) is large, on the order of 50, most of them are rigidly defined constants, whose values are assigned explicitly or implicitly from the fulfillment of various thermodynamic conditions at specific points on the phase diagram. A few coefficients (about 10) serve to characterize the densities and temperatures on transition from one typical phase-plane region to another and are found empirically. Basically, in constructing the EOS, the following information is used at high pressures, high temperatures: measurements of isothermal compressibility in diamond anvil cells (DAC), data on sound velocity and density in liquid metals at atmospheric pressure, isobaric expansion (IEX), or so-called "exploding wires" measurements, registration of shock compressibility for solid and porous samples in incident, and reflected shock waves, impedance measurements of shock compressibility under conditions of an underground nuclear explosion, data on isentropic expansion of shocked metals, calculations by Debay-Hukkel and Thomas-Fermi models, evaluations of the critical point, for more details see Lomonosov (2007).

The direct use of multi-phase EOS in computer codes leads to complicated and inefficient calculations, so they are usually involved in numerical modeling in tabular form. The EOS code for calculation of tables can produce the complete set of thermodynamic derivatives (such as pressure, sound velocity, heat capacity) using any one of input pairs: volume-temperature, volume-internal energy, or volume-pressure. The input grid can be linear, logarithmic, or arbitrary; each point in the two-dimensional output tables is marked by a symbol which indicates the physical state, namely, solid, liquid, gas, plasma, or mesh (solid-liquid, liquid-gas). Typical EOS three-dimensional pressure-volume-temperature surfaces for copper and tungsten are presented in Figures 3 and 4, respectively. In these Figures, as seen on the phase surfaces, a complete set of available high-pressure, high temperature data together with phase boundaries, and physical states generated by intense SPS proton beams. One should especially emphasize that intense SPS beams have the potential to produce unique physical states of matter, corresponding to the domain occupied by strongly coupled plasma (Fortov

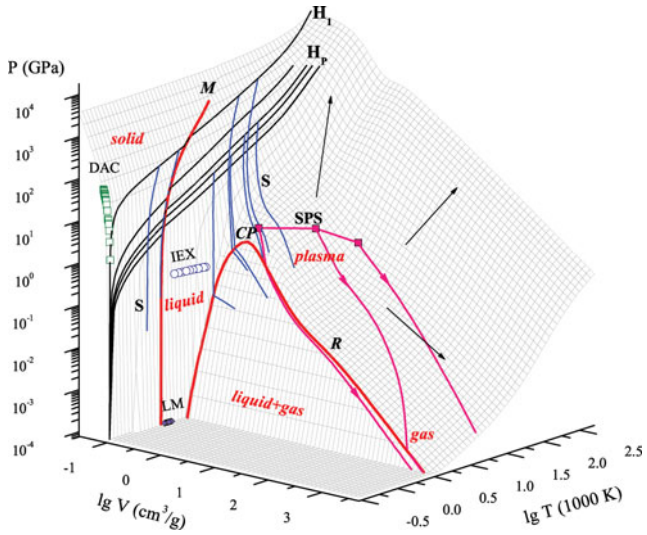

Fig. 3. (Color online) 3D pressure-volume-temperature surface for copper. Nomenclature: M - melting region; R - evaporating region with the critical point, CP; solid, liquid, gas, liquid + gas and plasma (arrows indicate the decrease of plasma non-ideality parameter) - physical states; H_1 and H_p - principal and porous Hugoniots, S - release isentropes of shock-compressed metal; IEX - isobaric expansion ("exploding wires") data; DAC - static compression in diamond anvil cells; LM - density of liquid metal at room pressure; SPS - states in copper, generated by intense SPS proton beams in the center of the target at the end of pulses (points correspond to deposited energies of 8.13, 19.3 and 41.4 kJ/g) and during subsequent expansion of metal, bold curves with arrows).

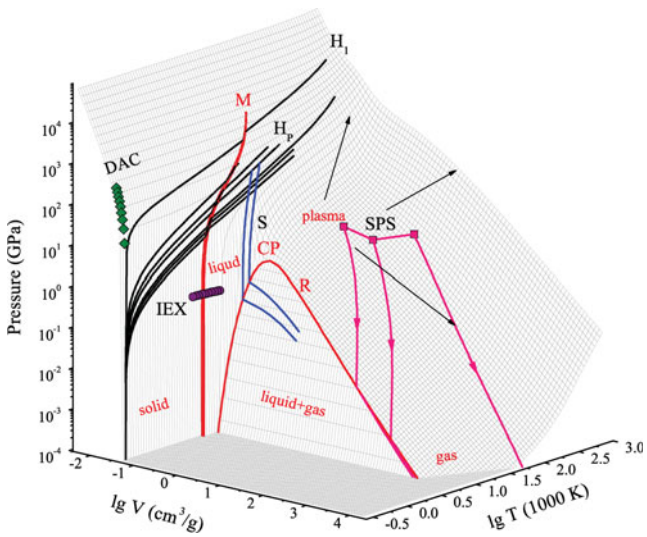

Fig. 4. (Color online) 3D pressure-volume-temperature surface for tungsten. Nomenclature: M - melting region; R - evaporating region with the critical point, CP; solid, liquid, gas, liquid + gas and plasma (arrows indicate the decrease of plasma non-ideality parameter) - physical states; H_1 and H_p - principal and porous Hugoniots, S - release isentropes of shock-compressed metal; IEX - isobaric expansion ("exploding wires") data; DAC - static compression in diamond anvil cells; SPS - states in tungsten, generated by intense SPS proton beams in the center of the target at the end of pulses (points correspond to deposited energies of 17.3, 25.2 and 111.3 kJ/g) and during subsequent expansion of metal, bold curves with arrows).

et al., 1999). Such experiments will give a nice opportunity to put reference points in the domain of the phase diagram which is traditionally very difficult to access and which is also difficult for pure theoretical description even with use of advanced modern theories.

Recently, a modified quotidian EOS model that provides improved treatment of the low density region of the phase diagram, has been reported (Ray *et al.*, 2006).

5. NUMERICAL SIMULATION RESULTS

5.1. Beam and target parameters

We consider a full SPS beam that is composed of 288 proton bunches. Each bunch consists of 1.1×10^{11} protons with a duration of 0.5 ns while two neighboring bunches are separated by 25 ns so that the total length of the pulse is about 7 μs.

Intensity distribution in transverse direction is assumed to be Gaussian and three different values for the beam focal spot with a standard deviation, $\sigma = 0.088$ mm, 0.28 mm, and 0.88 mm, respectively, have been considered in this study. The beam is incident on the face of the cylindrical target.

The protons and the secondary particles penetrate into the target and specific energy deposition by one proton bunch on copper and tungsten targets along the beam direction is shown in Figures 1a and 2a, respectively. The specific energy deposition in transverse direction at maximum value along the length is plotted in Figures 1b and 2b, respectively. In the hydrodynamic simulations, we consider a cross section of the cylinder at the point of maximum energy deposition and study the target behavior in the transverse direction.

In the following, we present the numerical simulation results of thermodynamic and hydrodynamic response of two targets made of solid copper and solid tungsten, respectively.

5.2. Copper target

Numerical simulations have shown that at the end of the SPS pulse, specific energy of 41.4 kJ/g, 19.3 kJ/g, and 8.23 kJ/g is deposited for the beam focal spot, $\sigma = 0.088$ mm, 0.28 mm, and 0.88 mm, respectively.

In Figures 5a–5c, respectively, we plot temperature, pressure, and density versus target radius at the end of the pulse. It is seen that in case of a focal size with $\sigma = 0.088$ mm, a temperature of about 45000 K is generated at the target center where as for the cases with $\sigma = 0.28$ mm and 0.88 mm, the corresponding temperature is 25000 K and 10000 K, respectively.

The high temperature generates a strong radial outgoing shock wave that moves material outward that reduces the density at the target center. The pressure curves (Fig. 5b) for the three values of σ at the end of the pulse (at about

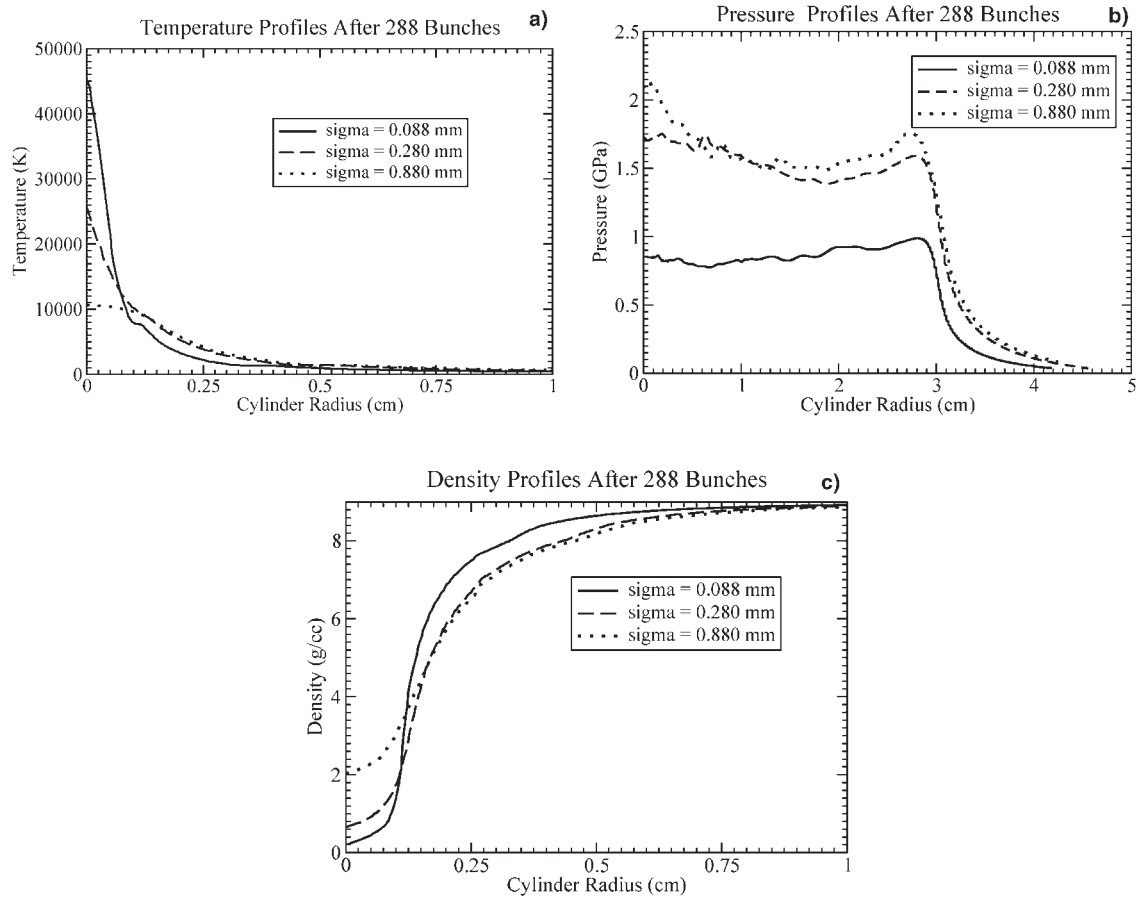

Fig. 5. Solid copper cylinder irradiated with SPS beam comprised of 288 proton bunches, bunch length = 0.5 ns, bunch separation = 25 ns, number of protons in one bunch = 1.1×10^{11}, Gaussian particle distribution in transverse direction with three values of σ = 0.088 mm, 0.28 mm, and 0.88 mm, respectively; (**a**) temperature versus radius, (**b**) pressure versus radius, and (**c**) density versus radius, at the end of the pulse.

7 μs) show that the pressure has a behavior opposite to the temperature as the pressure curve with $\sigma = 0.088$ mm lies at the lowest position. This is because the material density is the lowest for this case (see Fig. 5c).

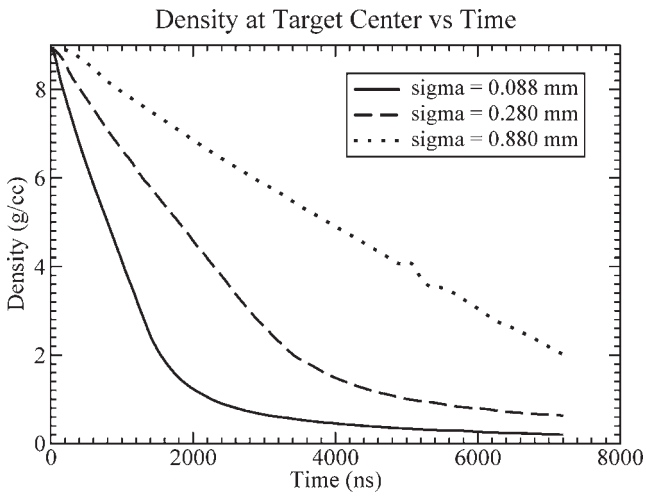

Fig. 6. Density at center of copper target versus time.

Figure 6 shows the variation in density at the target center as a function of time. It is seen that the density decreases by an order of magnitude in first 2 μs for the case, $\sigma = 0.088$ mm that means that the protons delivered in subsequent bunches will penetrate further into the target (tunnel effect). The density reduction also takes place for the other two values of σ, although it is not so substantial as in the former case.

It is seen from Figures 5a–5c that the physical conditions within about 1 mm from the target axis, correspond to a strongly coupled plasma state that is surrounded by a region of compressed hot liquid.

5.3. Tungsten target

According to the numerical simulations, specific energy of 111.3 kJ/g, 25.2 kJ/g, and 17.3 kJ/g is deposited by the full SPS beam corresponding to beam focal spot with $\sigma = 0.088$ mm, 0.28 mm, and 0.88 mm, respectively.

Figures 7a–7c show simulation results using a solid tungsten target that are plotted at the end of the proton pulse (at about 7 μs). It is seen from Figure 7a that the target center is heated to a maximum temperature of about

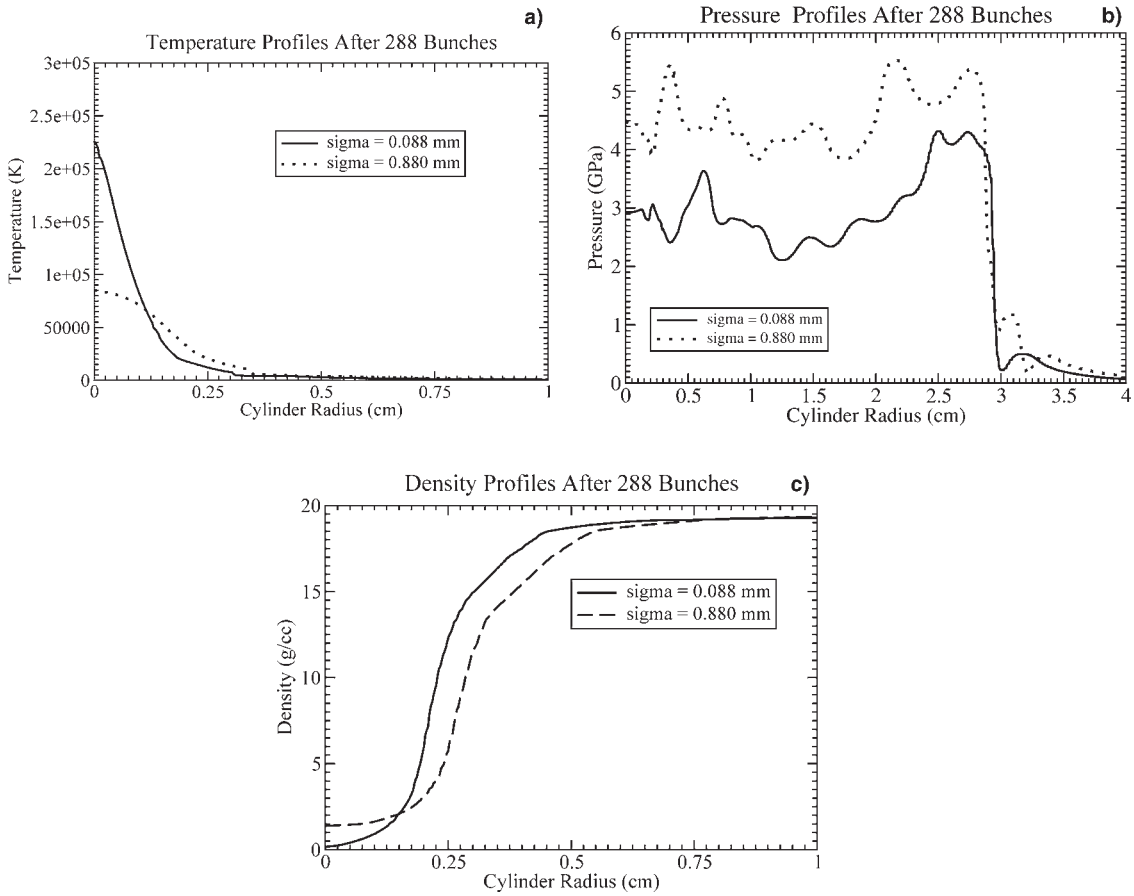

Fig. 7. Solid tungsten cylinder irradiated with SPS beam comprised of 288 proton bunches, bunch length = 0.5 ns, bunch separation = 25 ns, number of protons in one bunch = 1.1×10^{11}, Gaussian particle distribution in transverse direction with three values of σ = 0.088 mm, and 0.88 mm, respectively; (**a**) temperature versus radius, (**b**) pressure versus radius, and (**c**) density versus radius, at the end of the pulse.

200000 K for the case with σ= 0.088 mm while the for σ = 0.88 mm one has a lower value of 80000 K. Again in Figure 7b, the pressure curve shows a behavior opposite to that of the temperature (pressure values for $\sigma = 0.88$ mm are higher than for $\sigma = 0.088$ mm). This is because the density corresponding to $\sigma = 0.088$ mm is much lower than that in case of $\sigma = 0.88$ mm. The density versus time at the center of tungsten target is shown in Figure 8. One sees a behavior similar to that seen in Figure 6.

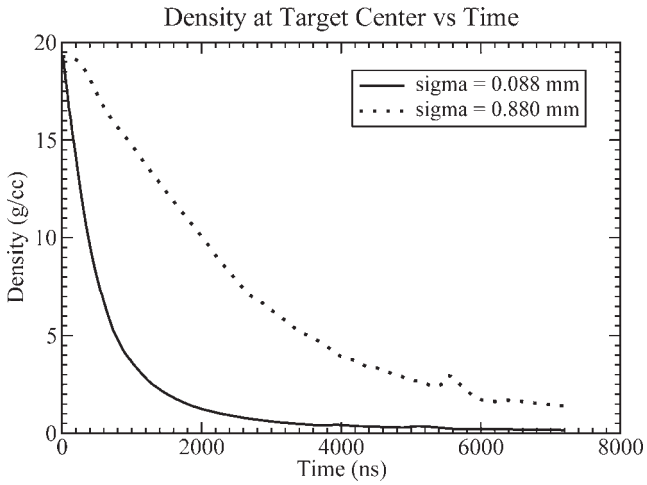

Fig. 8. Density at center of tungsten target versus time.

6. CONCLUSIONS

We have carried out numerical simulations of the interaction of a full SPS 450 GeV/c proton beam with solid copper and tungsten targets. The beam consists of 288 proton bunches, each with 1.1×10^{11} protons, bunch length = 0.5 ns and two neighboring bunches are separated by 25 ns and thus the total length of the pulse is about 7 μs. The particle distribution in the transverse direction is assumed to be a Gaussian and three different focal spot sizes have been considered: $\sigma = 0.088$ mm, 0.28 mm, and 0.88 mm, respectively.

The energy deposition by the protons together with the secondary particles has been evaluated using the FLUKA code and this energy deposition data has been used as input to the hydrodynamic code BIG-2. These simulations have clearly shown that an accident involving impact of a

full SPS beam can cause considerable damage to the equipment. Due to reduction in density caused by hydrodynamics induced as a result of beam heating, the protons delivered in subsequent bunches will penetrate deeper into the target, thereby increasing the effective particle range. This has an important consequence for LHC machine protection in case of an accident. Tests at SPP will allow validating these effects. Finally, the SPS can also be used to study high energy density states in matter.

ACKNOWLEDGEMENT

This work was financially supported by the BMBF, Germany and RFBR grant No.06-02-04011-NNIOa, Russia.

REFERENCES

Bushman, A.V., Kanel, G.I., Ni, A.L. & Fortov, V.E. (1993). *Thermophysics and Dynamics of Intense Pulsed Loadings.* London: Taylor and Francis.

Fasso, A., Ferrari, A., Roesler, S., Sala, P.R., Battistoni, G., Cerutti, F., Gadioli, E., Garzelli, M.V., Ballarini, F., Ottolenghi, A., Empl, A. & Ranft, J. (2003). The physics models of FLUKA: Status and recent developments. http://arxiv.org/PS_cache/hep-ph/pdf/0306/0306267v1.pdf.

Fasso, A., Ferrari, A., Ranft, J. & Sala, P.R. (2005). FLUKA: A multiparticle transport code. http://aliceinfo.cern.ch/alicvs/viewvc/doc/fluka.slac-r-773.pdf?revision=1.2.

Fortov, V.E., Goel, B., Munz, C.-D., Ni, A.L., Shutov, A. & Vorbiev, O.Yu. (1996). Numerical simulations of non-stationary fronts and interfaces by the Godunov method in m oving grids. *Nucl. Sci. Eng*. **123**, 169.

Fortov, V.E. & Yakubov, I.T. (1999). *Physics of Non-Ideal Plasmas*. London: World Science Publishers.

Goddard, B., Kain, V., Uythoven, J. & Wenninger, J. (2004). TT40 damage during 2004 high intensity SPS extraction. CERN-AB-Note-2005-014, Geneva.

Hoffmann, D.H.H., Blazevic, A., Ni, P., Rosmej, O., Roth, M., Tahir, N.A., Tauschwitz, A., Udrea, S., Varentsov, D., Weyrich, K. & Maron, Y. (2005). Present and future perspectives of high energy density physics with intense ions and laser beams. *Laser Part. Beams* **23**, 47.

Kain, V., Vorderwinkler, K. Ramillon, J., Schmidt, R. & Wenninger, J. (2005). Material damage test with 450 GeV LHC-type beam. http://accelconf.web.cern.ch/accelconf/p05/papers/rppe018.pdf.

Lomonosov, I.V. (2007). Multi-phase equation of state for aluminum. *Laser Part. Beams* **25**, 567–584.

Lopez Cela, J.J., Piriz, A.R., Serena Moreno, M. & Tahir, N.A. (2006). Numerical simulations of Rayleigh–Taylor instability in elastic solids. *Laser Part. Beams* **24**, 427.

Piriz, A.R., Portugues, R.F., Tahir, N.A. & Hofmann, D.H.H. (2002). Implosion of multilayered cylindrical targets driven by intense heavy ion beams. *Phys. Rev. E.* **66**, 056403.

Piriz, A.R., Temporal, M., Lopez Cela, J.J., Tahir, N.A. & Hoffmann, D.H.H. (2003*a*). Symmetry analysis of cylindrical implosions driven by high-frequency rotating ion beams. *Plasma Phys. Contr. Fusion* **45**, 1733.

Piriz, A.R., Tahir, N.A., Hoffmann, D.H.H. & Temporal, M. (2003*b*). Generation of hollow ion beam: calculation of rotation frequency required to accommodate symmetry constraints. *Phys. Rev. E.* **67**, 017501.

Piriz, A.R., Lopez Cela, J.J., Cortazar, O.D., Tahir, N.A. & Hoffmann, D.H.H. (2005). Rayleigh-Taylor instability in elastic solids. *Phys. Rev. E.* **72**, 056313.

Piriz, A.R., Lopez Cela, J.J., Serena Moreno, M., Tahir, N.A. & Hoffmann, D.H.H. (2006). Thin plate effects in the Rayleigh-Taylor instability of elastic solids. *Laser Part. Beams* **24**, 275.

Piriz, A.R., Tahir, N.A., Lopez Cela, J.J., Cortazar, O.D., Serna Moreno, M.C., Temporal, M. & Hoffmann, D.H.H. (2007*a*). Analytic models for the design of the LAPLAS target. *Contrib. Plasma Phys.* **47**, 213.

Piriz, A.R., Lopez Cela, J.J., Serna Moreno, M.C., Cortazar, O.D., Tahir, N.A. & Hoffmann, D.H.H. (2007*b*). A new approach to Rayleigh–Taylor instability: Applications to accelerated elastic solids. Nucl. Instrum. *Meth. Phys. Res. A.* **577**, 250.

Ray, A., Srivastava, M.K., Kodayya, G. & Menon, S.V.G. (2006). Improved equation of state of metals in the liquid-vapor region. *Laser Part. Beams* **24**, 437.

Tahir, N.A., Hoffmann, D.H.H., Maruhn, J.A., Spiller, P. & Bock, R. (1999). Heavy ion induced hydrodynamic effects in solid targets. *Phys. Rev. E.* **60**, 4715.

Tahir, N.A., Hoffmann, D.H.H., Kozyreva, A., Shutov, A., Maruhn, J.A., Neuner, U., Tauschwitz, A., Spiller, P. & Bock, R. (2000*a*). Shock compression of condensed matter using intense beams of energetic heavy ions. *Phys. Rev. E.* **61**, 1975.

Tahir, N.A., Hoffmann, D.H.H., Kozyreva, A., Shutov, A., Maruhn, J.A., Neuner, U., Tauschwitz, A., Spiller, P. & Bock, R. (2000*b*). Equation-of-state properties of high-energy-density matter using intense heavy ion beams with an annular focal spot. *Phys. Rev. E.* **62**, 1224.

Tahir, N.A., Kozyreva, Spiller, P., Hoffmann, D.H.H. & Shutov, A. (2001*a*). Necessity of bunch compression for heavy-ion-induced hydrodynamics and studies of beam fragmentation in solid targets at a proposed synchrotron facility. *Phys. Rev. E.* **63**, 036407.

Tahir, N.A., Hoffmann, D.H.H., Kozyreva, A., Tauschwitz, A., Shutov, A., Maruhn, J.A., Spiller, P., Nuener, U., Jacoby, J., Roth, M., Bock, R., Juranek, H. & Redmer, R. (2001*b*). Metallization of hydrogen using heavy-ion-beam implosion of multi-layered targets. *Phys. Rev. E.* **63**, 016402.

Tahir, N.A., Juranek, H., Shutov, A., Redmer, R., Piriz, A.R., Temporal, M., Varentsov, D., Udrea, S., Hoffmann, D.H.H., Deutsch, C., Lomonosov, I. & Fortov, V.E. (2003*a*). Influence of the equation of state on the compression and heating of hydrogen. *Phys. Rev. B.* **67**, 184101.

Tahir, N.A., Shutov, A., Varentsov, D., Spiller, P., Udrea, S., Hoffmann, D.H.H., Lomonosov, I.V., Wieser, J., Kirk, M., Piriz, R., Fortov, V.E. & Bock, R. (2003*b*). Influence of the equation of state of matter and ion beam charesteristics on target heating and compression. *Phys. Rev. Spec. Topics Accel. Beams* **6**, 020101.

Tahir, N.A., Goddard, B., Kain, V., Schmidt, R., Shutov, A., Lomonosov, I.V., Piriz, A.R., Temporal, M., Hoffmann, D.H.H. & Fortov, V.E. (2005*a*). Impact of 7-Tev/c large

hadron collider proton beam on a copper target. *J. Appl. Phys*. **97**, 083532.

Tahir, N.A., Kain, V., Schmidt, R., Shutov, A., Lomonosov, I.V., Gryaznov, V., Piriz, A.R., Temporal, M., Hoffmann, D.H.H. & Fortov, V.E. (2005*b*). The CERN large hadron collider as a tool to study high-energy-density physics. *Phys. Rev. Lett*. **94**, 135004.

Tahir, N.A., Adonin, A., Deutsch, C., Fortov, V.E., Grandjouan, N., Geil, B., Gryaznov, V., Hoffmann, D.H.H., Kulish, M., Lomonosov, I.V., Mintsev, V., Ni, P., Nikolaev, D., Piriz, A.R., Shilkin, N., Spiller, P., Shutov, A., Temporal, M., Ternovoi, V., Udrea, S. & Varentsov, D. (2005*c*). Studies of heavy ion-induced highenergy density states in matter at the GSI Darmstadt SIS-18 and future FAIR facility. *Nucl. Instrum. Meth. Phys. Res. A*. **544**, 16.

Tahir, N.A., Deutsch, C., Fortov, V.E., Gryaznov, V., Hoffmann, D.H.H., Kulish, M., Lomonosov, I.V., Mintsev, V., Ni, P., Nikolaev, D., Piriz, A.R., Shilkin, N., Spiller, P., Shutov, A., Temporal, M., Ternovoi, V., Udrea, S. & Varentsov, D. (2005*d*). Proposal for the study of thermophysical properties of high-energy-density matter using current and future heavy ion accelerator facilities at GSI Darmstadt. *Phys. Rev. Lett*. **95**, 035001.

Tahir, N.A., Spiller, P., Udrea, S., Cortazar, O.D., Deutsch, C., Fortov, V.E., Gryaznov, V., Hoffmann, D.H.H., Lomonosov, I.V., Ni, P., Piriz, A.R., Shutov, A., Temporal, M. & Varentsov, D. (2006). Studies of equation-of-state properties of high-energy density matter using intense heavy ion beams at the future FAIR facility: The HEDgeHOB Collaboration. *Nucl. Instrum. Meth. Phys. Res. B*. **245**, 85.

Tahir, N.A., Spiller, P., Shutov, A., Lomonosov, I.V., Gryaznov, V., Piriz, A.R., Wouchuk, G., Deutsch, C., Fortov, V.E., Hoffmann, D.H.H. & Schmidt, R. (2007*a*). HEDgeHOB: High-energydensity matter generated by heavy ion beams at the future facility for antiprotons and ion research. *Nucl. Instrum. Meth. Phys. Res. A*. **577**, 238.

Tahir, N.A., Piriz, A.R., Shutov, A., Lomonosov, I.V., Gryaznov, V., Wouchuk, G., Deutsch, C., Spiller, P., Fortov, V.E., Hoffmann, D.H.H. & Schmidt, R. (2007*b*). Survey of theoretical work for the proposed HEDgeHOB collaboration: HIHEX and LAPLAS. *Contrib. Plasma Phys*. **47**, 223.

Tahir, N.A., Kim, V., Grigoriev, D.A., Piriz, A.R., Weick, H., Geissel, H. & Hoffmann, D.H.H. (2007*c*). High energy density physics problems related to liquid jet lithium target for Super-FRS fast extraction scheme. *Laser Part. Beams* **25**, 295.

Temporal, M., Piriz, A.R., Grandjouan, N., Tahir, N.A. & Hoffmann, D.H.H. (2003). Numerical analysis of a multilayered cylindrical target compression driven by a rotating intense heavy ion beam. *Laser Part. Beams* **21**, 609.

Temporal, M., Lopez-Cela, J.J., Piriz, A.R., Grandjouan, N., Tahir, N.A. & Hoffmann, D.H.H. (2005). Compression of a cylindricalhydrogen sample driven by an intense co-axial heavy ion beam. *Laser Part. Beams* **23**, 137.